OGLE-2007-BLG-050 : Detection efficiency to planetary companion with finite source and parallax effects

V. Batista[1], S. Dong[2], A. Gould[2], JP. Beaulieu[1], A. Cassan[3]

[1] Institut d'Astrophysique de Paris, 98Bis Boulevard Arago, 75014 Paris, France, (batista@iap.fr, beaulieu@iap.fr)

[2] Department of Astronomy, Ohio State University, 140 WEST 18th Avenue, Colombus, OH 43210 (dong@astronomy.ohio-state.edu, gould@astronomy.ohio-state.edu)

[3] Astronomisches Rechen-Institut, MönchofStr. 12-14, 69120 Heidelberg, Germany (cassan@ari.uni-heidelberg.de)

1. Introduction

We analyze OGLE-2007-BLG-050, a high magnification microlensing event ($A_{max} = 432$) which peak occured on May, 1, 2007, with pronounced finite-source effects. We compute detection efficiency on this event to see its sensitivity to the presence of planets around the lens star, following the method proposed by Gaudi & Sackett (2000) and used in particular by Gaudi et al. 2002 and Cassan et al. 2008 (in prep.). Both finite-source and parallax effects permit a measurement of the angular Einstein radius θ_E and the parallax π_E, leading to an estimate of the lens mass M and its distance to the observer D_L. The detection efficiency diagram in the physical space $(\tilde{r}, m_p)$, where m_p is the mass planet and $\tilde{r}$ the projected separation with the lens, can then be built.

2. Observational data and extended-source point-lens fit

This microlensing event was identified by the OGLE III Early Warning System (EWS; Udalski 2003) and was monitored by Microlensing Follow-Up Network (µFun; Yoo et al. 2004) and by Probing Lensing Anomalies Network (PLANET; Albrow et al. 1998). The following study is based on the µFun data from New Zealand, South Africa, Chile and USA, in I and R bands, and on the OGLE data and the MOA data in I band.

The ***Fig. 1*** shows the extended-source point lens fit (ESPL) obtained following the formalism given by Yoo et al. (2004) for the finite-source effects and Gould (2004) for modeling parallax in the geocentric frame. 3-σ outliers from data points have been removed and the errors on data have been renormalized for each observatory so that the χ^2 per degree of freedom for the best-fit ESPL model is close to unity.

The principal parameters derived from the ESPL fit are : $u_0 = 0.00212$, $t_0 = 4221.97$ (HJD'), $t_E = 67.1$ days, $\rho_* = 0.00457$.

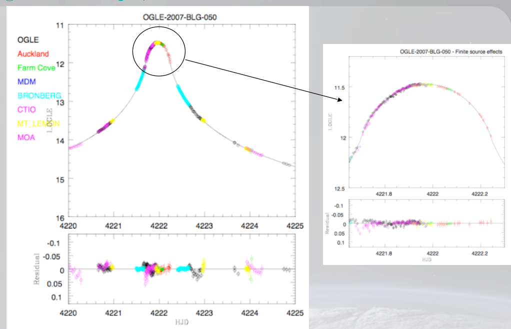

Fig. 1 : Light curve of OGLE-2007-BLG-050 near its peak on 2007 May 1

3. Binary lens models and detection efficiency

To characterize the planetary detection efficiency of OGLE-2007-BLG-050, we follow the Gaudi & Sackett (2000) method which consists in fitting binary models with the 3 binary parameters (d,q,α) held fixed (d : planet-lens separation in units of θ_E, q : planet-star mass ratio, α : angle of the source trajectory relative to the binary axis). To perform the calculations of binary light curves, we use a binary-lens finite-source algorithm developped by Dong et al. (2006) (Appendix A). The resulting grids of χ^2 as a function of d and α are shown in ***Fig. 2*** for some values of q.

The ensemble of (d,q,α) for which $\Delta\chi^2 = \chi^2(d,q,\alpha) - \chi^2_{ESPL} > \chi^2_C = 60$ is said to be excluded for that event. For each (d,q), the fraction of angles $0 \le \alpha \le 2\pi$ that was excluded was designated the « sensitivity » for that system. Indeed, the detection efficiency $\varepsilon(d,q)$ can be expressed as :

$$\varepsilon(d,q) = \frac{1}{2\pi}\int_0^{2\pi}\Theta\left(\Delta\chi^2(d,q,\alpha) - \chi^2_C\right)\, d\alpha \ ; \ \Theta : step \quad function$$

The resulting detection efficiency diagram for OGLE-2007-BLG-050 is shown on ***Fig. 3***. The part where $d < 1$ is derived from the one where $d > 1$ due to the degeneracy on d <-> $1/d$. This event seems to be sensitive to very low mass ratios with a high detection efficiency for q as low as 10^{-5} in range $[0.6, 1.6]$ of d.

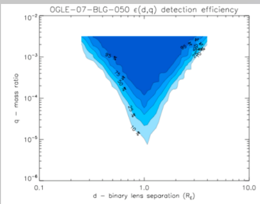

__Fig. 3__ : Resulting detection efficiency diagram for d and q ranges of [0.2 - 4] R_E and [$10^{-5.5}$-$10^{-2.5}$] M_{lens}. The part where d < 1 is derived from the one where d > 1 due to the degeneracy on d <-> 1/d. This approximation was used in this preliminary study but won't be assumed in a further analysis.

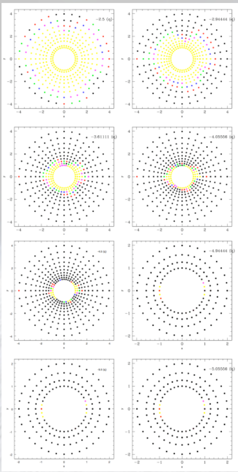

__Fig. 2__ Binary-lens finite-source grids of χ^2 as a function of (x,y), where x = dcosα and y = dsinα, for different q. The values that appear in the right upper part of each diagram correspond to log(q). The color thresholds are defined as : $\Delta\chi2 < 60$, 60 -100, 100 - 150, 150 - 200, 200 - 300, > 300, where $\Delta\chi2$ is the $\chi2$ difference between a given binary lens model and the ESPL fits. These diagrams have been computed for d and q ranges of [1 - 4] R_E and [$10^{-5.5}$-$10^{-2.5}$] M_{lens}, and for 36 values of α.

4. Source properties from Color-Magnitude Diagram and measurement of θ_E

To determine the dereddened color and magnitude of the microlensed source, we put the best fit instrumental color and magnitude of the source on an instrumental *(I,V-I)* CMD (***Fig. 4***).

The measured color and magnitude of the clump on that CM diagram is $(V,V\text{-}I)_{clump} = (17.20,0.00)$ (red dot). For the absolute color magnitude, we adopt the Hipparcos position $M_I = -0.23 \pm 0.03$ (Stanek & Garnavich (1998)). The mean Hipparcos clump color of $(V\text{-}I)_{0,clump} = 1.00 \pm 0.05$ is adopted. Assuming a Galactic center distance of $8kpc$, $\mu = 14.52 \pm 0.10$ and the magnitude of the clump is given by $I_{0,clump} = 14.29 \pm 0.13$. We derive $(I,V\text{-}I)_{0,clump} = (14.29,1.00) \pm (0.13,0.05)$. On the CMD, the apparent color and magnitude of the source are $(I,V\text{-}I) = (19.40,-0.12) \pm (0.08,0.05)$ (black dot on ***Fig. 4***). Hence, the dereddened source color and magnitude are given by : $(I,V\text{-}I)_0 = (16.49,0.88) \pm (0.21,0.10)$.

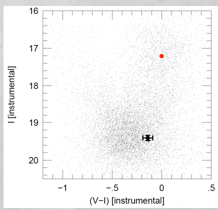

__Fig.4__ : Uncalibrated color-magnitude of the field around OGLE-07-BLG-050. The red dot is the red clump and the black filled circle is the µFun CTIO V and V-I measurements of the source with 1-σ error bars.

The color determines the relation between dereddened source flux and angular source radius. We use the following expression given by Kervella et al. (2004) for dwarf stars :

$$\log(\theta_*) = 3.212 - 0.2 I_0 + 0.421(V-I)_0, \quad and \quad \theta_* = 1.93 \pm 0.08 \quad \mu as$$

With the angular size of the source given by the ESPL fit, $\rho_* = 0.00457 \pm 0.00006$, we can derive the angular Einstein radius θ_E : $\theta_E = \theta_*/\rho_* = 0.42 \pm 0.02$ *mas*, and combined with the fitted timescale of the event $t_E = 67.1 \pm 0.9$ *days*, it gives the relative lens-source proper motion : $\mu = 2.3 \pm 0.1$ *mas/yr*.

5. Parallax effects - Lens mass and distance estimates

The long timescale of the event enables to obtain constraints on the microlens parallax. The ESPL fit yields to the determination of the components $(\pi_{E,N}, \pi_{E,E})$ of the parallax π_E projected on the sky in north and east celestial coordinates by maping a grid of χ^2 (***Fig. 5***). The magnitude of π_E is then : $\pi_E = 0.22 \pm 0.10$.

Gould (1992) showed that if both θ_E and π_E could be measured, then the mass and lens-source relative parallax could be determined :

$$M = \theta_E / \kappa\pi_E = 0.24 \pm 0.09 \ M_{sol} \quad with \quad \kappa = 4G/c^2 AU$$

$$\pi_{rel} = \pi_E \theta_E = 92 \pm 5 \quad \mu as$$

$$\pi_{rel} = 1AU\left(\frac{1}{D_L} - \frac{1}{D_S}\right); \ D_L = 4.6 \pm 0.1 \ kpc$$

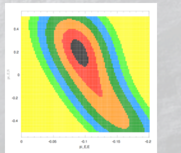

__Fig. 5__ : Likelihood contours as a function of the vector parallax π_E. The best fit is $\pi_E = (0.20,-0.09)$. There is a hard 3-σ lower limit $\pi_E > 0.075$ which implies $M < 0.7\ M_{sun}$ and $D_L < 6.4$ kpc.

6. Dectection efficiency diagram in physical units $(\tilde{r}, m_p)$

Having an estimate of the angular Einstein radius θ_E, the distance D_L of the lens from the observer and the lens mass M, we derive estimates of the physical parameters $(\tilde{r}, m_p)$ for the tested planetary models and calculate the associated detection efficiency, where $\tilde{r}$ is the projected separation between the planet and the star and m_p the planet mass.

$$\tilde{r}(AU) = d \ \ D_L(kpc) \ \ \theta_E(mas)$$
$$m_p = qM$$

The resulting detection efficiency diagram in physical units is shown in ***Fig. 6***. However the results presented here are still preliminary and need further confirmation (by eg. exploring a wider (d,q) grid in particular for $d < 1$ and higher q, denser in α), they demonstrate that OGLE-2007-BLG-050 is sensitive to Neptune-mass planets as well some Earth mass planets configurations.

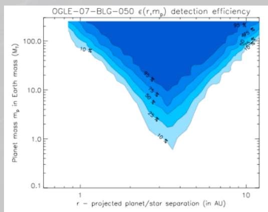

__Fig. 6__ : Detection efficiency diagram in physical units $(\tilde{r}, m_p)$. The contours indicate 10%, 25%, 50%, 75% and 95% efficiency.

7. Conclusion

OGLE-2007-BLG-050 is a high magnification event that presents the rare particularity to enable the measurement of finite source and parallax effects. This leads to an estimate of the angular Einstein radius θ_E, the mass M and distance D_L of the lens star. When computing planet detection efficiency $\varepsilon(d,q)$, it also permits to provide efficiency maps in physical space $\varepsilon(\tilde{r}, m_p)$, where $\tilde{r}$ is the projected planet/star seperation and m_p is the planet mass. Here we show that this microlensing event is sensitive to Neptune-mass planets and has some sensitivity to Earth-mass planets. We need to confirme these preliminary results by further analysis, to provide denser detection efficiency maps, and for example to compare these results to some obtained by Galactic models.

References

Albrow, M.D., et al. 1998, ApJ, 509, 687
Cassan, A., et al. 2008, A&A, 4414 (in prep.)
Dong, S., et al. 2006, ApJ, 642, 842
Gaudi, B.S. & Sackett, P.D. 2000, ApJ, 566, 463
Gaudi, B.S., et al. 2002, ApJ, 566, 463
Gould, A. 1992, ApJ, 392, 442
Gould, A. 2004, ApJ, 606, 319
Kervella, P., et al. 2004, A&A, 426, 297
Stanek, K.Z. & Garnavich, P.M. 1998, A&AS, 30, 1409
Udalski, A. 2003, Acta Astron., 53, 291
Yoo, J., et al. 2004, ApJ, 603, 139

Microlensing Manchester Conference 2008